DOI 10.1007/s11141-017-9760-8
Radiophysics and Quantum Electronics, Vol. 59, No. 11, April, 2017
(Russian Original Vol. 59, No. 11, November, 2016)

SIMULATION OF NONRELATIVISTIC JET EJECTIONS DURING THE LABORATORY STUDIES

**V. S. Beskin,[1,2*] Ya. N. Istomin,[1,2] A. M. Kiselev,[1,2]
V. I. Krauz,[3] K. N. Mitrofanov,[4] V. V. Myalton,[3]
E. E. Nokhrina,[2] D. N. Sob'yanin,[1] and
A. M. Kharrasov[3]**

UDC 533.9.072

We discuss a possibility of simulating nonrelativistic jet ejections during the laboratory experiment using the PF-3 facility. It is shown that many properties of the flows obtained with the help of the experimental facility agree with the basic characteristics of the jet ejections which are observed in the neighborhood of young stars. The future experiments, which can allow one to understand the nature of the stable plasma ejections observed in many astrophysical sources, are discussed.

1. INTRODUCTION

At an early stage of their evolution prior to reaching the main sequence, the stars (young stars) are in the accretion stage [1]. In this case, two well collimated supersonic jet ejections (jets) whose material velocity attains several hundred kilometers per second are usually observed for the majority of such stars. When interacting with the surrounding medium, the jets create shock waves, which were discovered in the 1950s as bright spots called the Herbig–Haro objects. The characteristic longitudinal and transverse sizes of these jets can reach several parsecs and several tens of astronomical units, respectively.

Recall that the jet ejections are observed for various different space sources from blazars, active galactic nuclei, and, presumably, gamma-ray bursts to microquasars[1] and young stars. The jets in these objects have scales from megaparsecs (active galactic nuclei) to several parsecs (young stars) and velocities from ultrarelativistic with a Lorentz factor of several tens to nonrelativistic (young stars) values. In this case, the jet injections allow the stars to naturally dispose of their excess angular momenta and the accretion material, which makes it possible for a young star to be compressed to the required size [2, 3]. The recent high-resolution observations are indicative of the jet rotation [4, 5], which confirms this hypothesis. Indeed, the axisymmetric Doppler shift in the direction normal to the jet axis is explained by the presence of a regular toroidal velocity of about 10–30 km/s.

It is natural that the angular-momentum loss is accompanied by an efficient energy release. In this case, the magnetohydrodynamic (MHD) model is the most suitable one for explaining the observed energy release and formation of the highly collimated jets outflowing from the star–accretion disk system, since it is exactly a regular magnetic field that determines the preferred direction of the jet ejection.

* beskin@lpi.ru

[1] Binary systems in our galaxy in which the mass flows over from a usual star to the neutron star or a black hole in the propeller mode.

[1] P. N. Lebedev Physical Institute of the Russian Academy of Sciences, Moscow; [2] Moscow Institute of Physics and Technology, Dolgoprudny; [3] Research Center "Kurchatov Institute," Moscow; [4] Troitsk Institute of Innovative and Thermonuclear Research, Troitsk, Russia. Translated from Izvestiya Vysshikh Uchebnykh Zavedenii, Radiofizika, Vol. 59, No. 11, pp. 1004–1016, November 2016. Original article submitted July 11, 2016; accepted September 12, 2016.

Of course, the collimation mechanism is the main issue within the framework of this model. In the nonrelativistic case, this problem was actively discussed within the framework of both the analytical self-similar [3, 6–9] and numerical [10–12] methods. At the same time, one can sometimes disregard the very issue of collimation and study the internal structure and stability of the already stationary supersonic jet ejections. This allows us to significantly simplify the MHD simulation. Once it is assumed that the flux is already collimated, the estimate based on the simplest assumption of the magnetic-flow conservation yields reasonable values for the transverse size $r_{\rm jet}$ of the jets in young stars. Actually, assuming that the outer-medium pressure plays the main role in the balance of forces, we write

$$r_{\rm jet} \sim R_{\rm in} \left(\frac{B_{\rm in}}{B_{\rm ext}} \right)^{1/2}, \tag{1}$$

where $R_{\rm in}$ is the size of the "central machine" and $B_{\rm in}$ and $B_{\rm ext}$ are the magnetic-field values near the star and external magnetic field, respectively. Since for the young stars with the radius $R_\odot$ we assume $B_{\rm in} \sim 10^2$–10^3 G, $R_{\rm in} \sim R_\odot$, and $B_{\rm ext} \sim 10^{-5}$–10^{-6} G, we obtain $r_{\rm jet} \sim 10^{15}$ cm, which agrees with the observation data. This means that the environment really plays an important role in the balance of forces of the already collimated jet [13–17].

The obvious complexity of the theoretical simulation of the astrophysical objects is related to the absence of the targeted experiments, which allow one to observe the system response by varying the physical parameters. In recent decades, such experiments have been replaced by numerical simulation which yielded important results [10–12]. At present, this tool is almost the only possible alternative to experiment when studying relativistic jet ejections.

At the same time, nonrelativistic ejections from the young stars can be simulated in a laboratory experiment with observation of certain similarity laws [18]. Such an approach is reasonable since the MHD equations, which govern both the astrophysical plasma jets and the laboratory-plasma flows, permit the spatial and temporal scaling. Considerable progress in simulating the astrophysical processes has been achieved in recent decades due to the appearance of a whole group of new facilities with high energy density, which were developed within the framework of the program of inertial controlled fusion [19]. In particular, the development of modern high-power lasers and Z-pinch systems made it possible to carry out well-controlled and well-diagnosable laboratory experiments on studying the hydrodynamic jets with high Mach numbers [20, 21].

A significant progress in the laboratory simulation of the astrophysical jets has also been attained using the MAGPIE facility (Imperial College London, Great Britain). During the experimental cycle, the rotation effects, which are discovered in the protostar jets, and interaction of the high-velocity radiation-cooled jets with the environment were simulated, possible mechanisms of the jet formation (e.g., "magnetic tower") were established, and other studies were performed [22–27]. Attractive results were obtained using the high-power laser at LULI laboratory (École Polytechnique), Paris, France) [28], which show that imposing the poloidal magnetic field can ensure efficient collimation of the plasma flow.

However, it should be noted that the above-mentioned experiments are mainly focused on the study of the jet-formation and jet-collimation processes. The jet dynamics was studied only on scales of about several centimeters. In this case, the jet-propagation process was almost disregarded, while the discharge of the fast Z-pinch type or the laser experiment were usually ensured by generating the plasma formations in a sufficiently high vacuum. At the same time, in the case of young stars, the hydrodynamic effects appearing during the jet propagation in the finite-density medium can be a significant factor.

Therefore, to simulate propagation of jets in the background plasma and study their stability, it should be possible to trace material propagation over significant distances compared with the transverse dimensions of the jets. The "plasma focus"-type facilities are very promising for achieving this goal [29]. Such facilities are known as the sources of intense plasma flows, which are widely used in various fields including simulation of various space phenomena [30]. The main experimental approaches to simulating the young-star jets within the framework of the above-formulated problems are discussed in this work.

2. BASIC PROPERTIES OF THE MHD MODEL

First of all, we should note a significant difference of the physical conditions, which are realized in the laboratory experiment, from the conditions in the actual astrophysical jet ejections. The fact is that the transverse size of the nonrelativistic jets from the young stars (several tens of astronomical units) by several orders exceeds the "central-machine" size. This means that the flow should be substantially expanded at the jet base, which leads to two conceptual consequences.

First, the expansion (also in the absence of additional heating, e.g., related to shock waves) should result in adiabatic cooling of the flow. Therefore, it is unlikely that the temperature effects in the actual jet ejections play a fundamental role. In addition, during the expansion, the flow should inevitably pass through the critical surfaces (Alfven's and magnetosonic surfaces), which determine the longitudinal current flowing along the jet and, thus, the total energy release in the system. However, in a laboratory experiment, the flow is weakly expanded during its propagation and, moreover, is substantially nonstationary.

Let us formulate the main properties of the MHD solutions, which underlie the majority of the models of the nonrelativistic jet ejections. In this case, special attention should be paid to their properties, which can be simulated in the laboratory experiment. Recall that the axisymmetric stationary flows (the observed astrophysical jet ejections satisfy these conditions with good accuracy) can conveniently be described using the "motion integrals," i.e., the quantities $\Psi = \text{const}$, where Ψ is the magnetic flux, which are preserved on the magnetic surfaces. Such quantities include the energy flux (Bernoulli integral) E_n being the sum of the energy flux of the particles and electromagnetic field (the Poynting vector), the angular-momentum flux L_n consisting of two parts, as well as the ratio η_n of the particle flux to the magnetic-field flux and the so-called "angular velocity of the field" Ω_F, which is actually specified by the rotational speed of the star and the accretion disc.

In this case, the following magnetization parameter characterizing the nonrelativistic flows is the main dimensionless parameter:

$$\sigma_\text{n} = \frac{\Omega_\text{F}^2 \Psi_\text{tot}}{8\pi^2 v_\text{in}^3 \eta_\text{n}}, \tag{2}$$

where Ψ_tot is the total magnetic flux passing through the "central machine" and the velocity v_in corresponds to the values of the flow velocity near the central object. Therefore, the slow-rotation condition $\sigma_\text{n} \ll 1$ corresponds to the limit of the weakly magnetized flow when the magnetic-field role in the total energy release is insignificant. On the contrary, the limit $\sigma_\text{n} \gg 1$ corresponds to the strongly magnetized flow when the electromagnetic processes play the main role. For the jet ejections from the young stars we have $\sigma_\text{n} \sim 10$–10^3 [31].

The first analytical solutions [14, 32, 33] showed that the flows with a zero total electric current for a constant angular velocity Ω_F do not exist. However, the solutions with zero current do exist if the angular velocity decreases to zero on the jet boundary and the external magnetic field and/or the gas pressure are not equal to zero [15, 34]. Such a formulation of the problem seems to be the most reasonable since it is assumed that the peripheral regions of the jet ejections are by the magnetic-field lines related to the external and, therefore, slowly rotating regions of the accretion discs, which presumably surround the young stars.

It is necessary to recall another important result, which was obtained for the axisymmetric supersonic flow. To make a reasonable choice of the angular-momentum $L_\text{n}(\Psi) \propto \Psi$ and the energy (Bernoulli integral) $E_\text{n}(\Psi) \approx \text{const}$ integrals for the magnetic flux $\Psi \ll \Psi_\text{tot}$ (i.e., near the rotation axis), the following dependence of the poloidal magnetic field B_p on the distance r to the rotation axis can be obtained:

$$B_\text{p} = \frac{B_0}{1 + r^2/r_\text{core}^2}, \tag{3}$$

where

$$r_\text{core} = v_\text{in}/\Omega_\text{F0}, \tag{4}$$

and the subscript 0 corresponds to the values on the rotation axis. This result was obtained for a cylindrical flow in both relativistic and nonrelativistic cases [35–37].

Note that the existence of the central region with a strong longitudinal magnetic field (3), and, thus, as was shown, a denser core leads to the fact that the outflowing current is concentrated in the central region $r < r_{\rm core}$ itself. Therefore, beyond the central region, the toroidal magnetic field should fall off as

$$B_\varphi \propto r^{-1}. \tag{5}$$

In this case, the current closure is assumed to occur only in the region of the so-called cocoon, i.e., the external casing of the ejection jet. Therefore, when discussing the laboratory experiment, one should pay special attention to the current closure in the peripheral regions of the jet ejection.

In the nonrelativistic case, the regularity condition on the fast magnetosonic surface requires that in the supersonic region (i.e., at a large distance from the "central machine") the electromagnetic-energy flux related to the Poynting vector $S = cE_r B_\varphi/(4\pi)$ is comparable with the kinetic energy $W_{\rm kin}$ of the outflowing plasma [31]. Therefore, the jet ejection should have a radial electric field whose value can be estimated as

$$E_r \approx \frac{4W_{\rm kin}}{cB_\varphi r_{\rm jet}^2}. \tag{6}$$

If the existence of the toroidal magnetic field B_φ in a laboratory experiment is doubtless, as is shown in what follows, the existence of the radial electric field E_r is not initially obvious. Therefore, the issue of the existence of the radial electric field should be studied in every detail.

Finally, as was noted, rotation of the astrophysical jet ejections is their key property. In this case, for sufficiently fast rotation (i.e., for $\sigma_{\rm n} \gg 1$), where the main energy near the "central machine" is transferred by the electric field, the simple relation [31]

$$W_{\rm tot} \approx \Omega_{\rm F}^{4/3}\, \Psi_{\rm tot}^{4/3}\, \dot{M}^{1/3} \tag{7}$$

exists between the total energy release $W_{\rm tot}$, the angular rotation speed $\Omega_{\rm F}$, the total magnetic flux $\Psi_{\rm tot}$ in the jet ejection, and the mass-loss rate $\dot{M}$. For known $W_{\rm tot}$, $\Psi_{\rm tot}$, and $\dot{M}$, this relation allows one to estimate the angular rotation speed. In this case, one should bear in mind that for the supersonic flows with $\mathcal{M} > 1$, where $\mathcal{M}$ is the Alfvén Mach number, the angular rotation speed Ω of plasma turns out to be a factor of $\mathcal{M}^2$ smaller than $\Omega_{\rm F}$. However, in this case it should be noted that the critical conditions on the singular surfaces were to a large extent used when deriving Eq. (7). Therefore, using this relationship to describe a laboratory experiment is not at all obvious. Nevertheless, the detected rotation would be an important confirmation of "similarity" of the laboratory experiment and the actual astrophysical jets.

3. EXPERIMENT DESCRIPTION

The above-formulated problems can be solved using the PF-3 facility of the Research Center "Kurchatov Institute" [29]. This facility is a plasma focus with the Filippov-type electrode geometry and one of the world-largest facilities of this type. The circuit diagram of the facility is shown in Fig. 1. The discharge chamber is a diode with the plane electrode geometry. The existing size of the discharge chamber, which is determined by the insulator size, allows the facility to be operated in the regimes optimized for obtaining a high plasma-compression degree for the voltage $U_0 = 8$–14 kV and the total current $I = 2$–3 MA. The characteristic time of the current build-up to the maximum value is about 10 μs.

The PF-3 plasma facility is operated as follows. After the preliminary pump-out, the chamber is filled with working gas (hydrogen, deuterium, helium, neon, argon, and their mixtures depending on the formulated tasks) under a pressure of a few torr. Once the discharge device of the facility is actuated, a high voltage appears between the orificed anode and cathode, which creates the working-gas breakdown along the insulator surface. Under the action of the Ampere force, the created current-carrying plasma shell

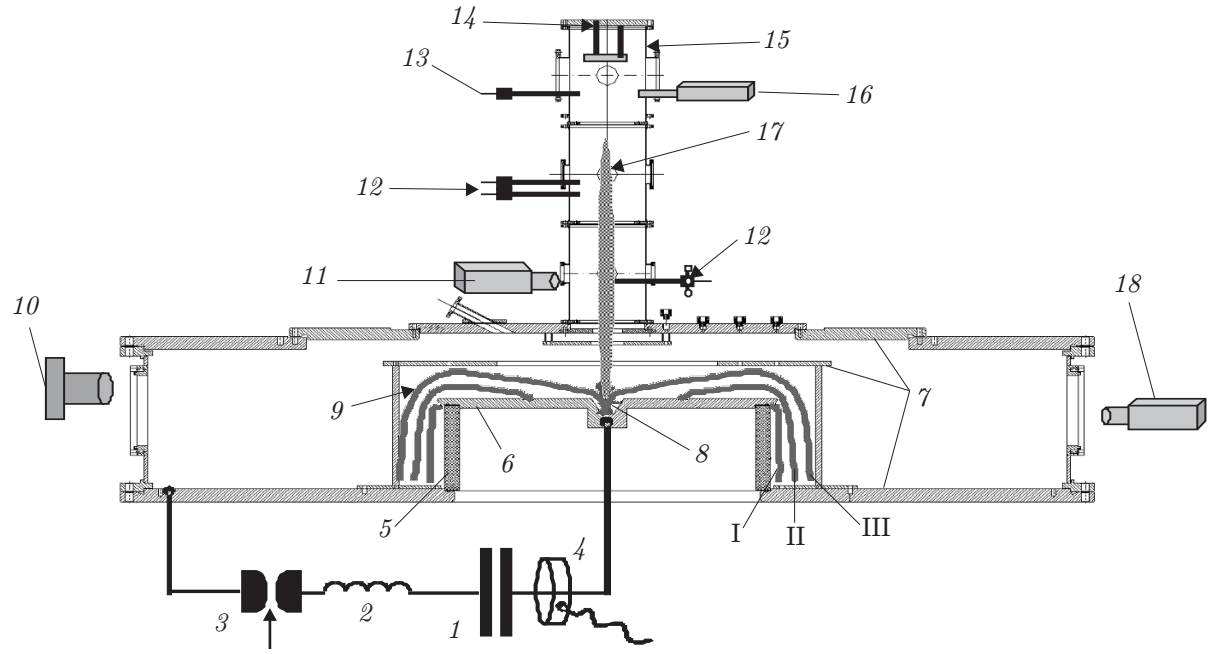

Fig. 1. The discharge chamber of the PF-3 facility and a set of diagnostic tools for studying the plasma flows: power supply (*1*), external inductance (*2*), discharge device (*3*), Rogowski coil (*4*), insulator (*5*), anode (*6*), cathode (*7*), pinch (*8*), current-carrying plasma shell (*9*), electron-optical transducer (*10*), electron-optical transducer, high-speed photographic recorder SFER-6, or spectroscopy unit (*11*), magnetic probe or optical collimator (*12*), optical collimator (*13*), ballistic pendulum and calorimeter (*14*), transit camera (*15*), laser diagnostics unit (*16*), jet (*17*), continuous strip cameras (*18*). Schematic image of the sequences of different discharge stages: breakdown phase (I), acceleration phase (II), the phase of the dense plasma focus (pinch) (III).

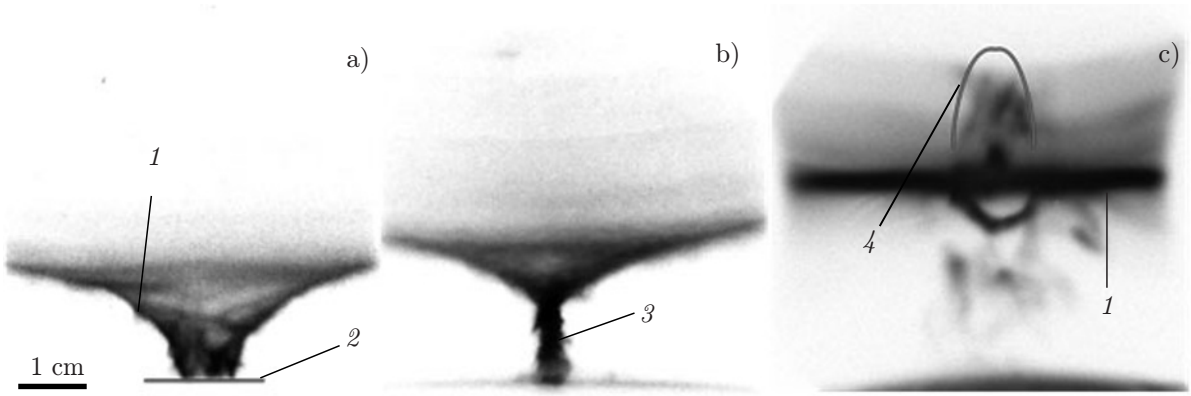

Fig. 2. Plasma-flow formation: the stage of convergence of the current-carrying plasma shell (*1*) to the axis (*a*), the pinch stage (*b*), the stage of the plasma-flow formation (*c*); anode (*2*), pinch (*3*), the plasma-flow front (*4*).

moves to the discharge axis on which the plasma pinching is observed.

The plasma pinch with a length of a few centimeters is formed near the anode and characterized by the temperature $T \sim 0.5$ keV and the density $N \sim 10^{19}\,\mathrm{cm}^{-3}$. In the dense-pinch stage, the current density exceeding $10^7\,\mathrm{A/cm}^2$ is reached, which leads to a build-up of strong current instabilities, the appearance of anomalous turbulent resistance, and an abrupt current breaking. Therefore, we have an effective plasma switch and the energy accumulated in the magnetic field of the pinch is transferred to the "load," i.e., an anomalous plasma heating and generation of the beams of the charged particles and intense neutron and

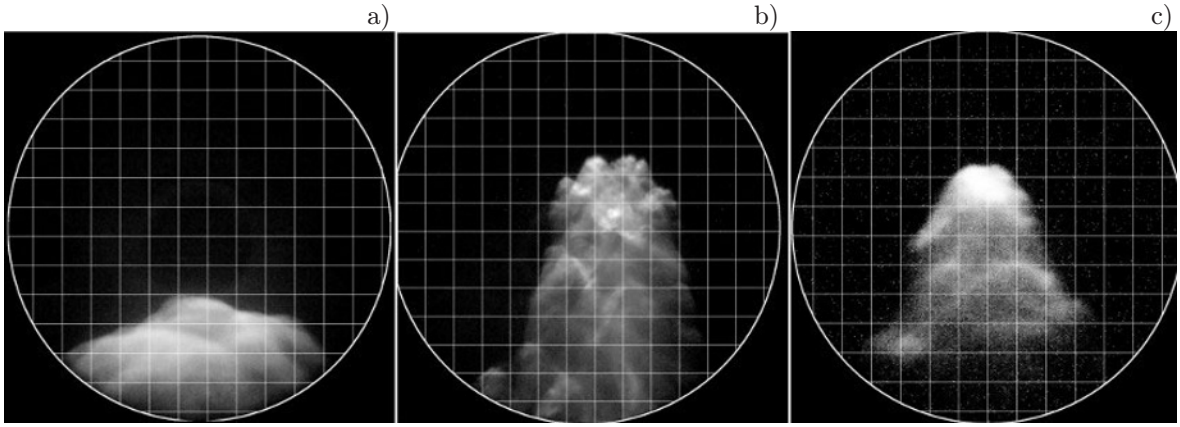

Fig. 3. Photographs of the plasma-flow front at the distance $z = 35$ cm from the anode for discharge in hydrogen (*a*) and neon (*b*), as well as in neon at a distance of 65 cm (*c*). The cell scale is 1 cm.

X-ray radiation occur. The characteristic time of the processes in this stage is from several to hundreds of nanoseconds. Then the development of the MHD instabilities leads to the pinch breakdown. In this stage, one can observe generation of intense plasma flows propagating along the system axis (see Fig. 2). The initial flow velocity is more than 10^7 cm/s, exceeds the motion velocity of the current-carrying plasma shell in the axial direction, and weakly depends on the working-gas type.

To study propagation of these flows, the PF-3 facility was upgraded [39, 40]. A new diagnostic drift chamber was developed, which allowed one to measure the jet and the surrounding-plasma parameters at distances of up to 100 cm from the plane of the anode, which was conventionally assumed to be the flow-generation region (see Fig. 1). In the estimates, the time corresponding to the peak value of the current derivative was assumed to be the generation time.

The chamber design allows one to both study the flow-generation processes in the anode region and measure the plasma-flow parameters at a significant distance. The chamber is equipped with a set of diagnostic windows with diameters ranging from 4 to 12 cm whose centers are located at distances of 35, 65, and 95 cm from the anode plane. Therefore, it is possible to study the flow-parameter dynamics at distances by two orders exceeding the initial transverse dimensions of the flow.

To study the flow parameters, a set of numerous diagnostic tools was used. The plasma-flow visualization using high-speed photographic recorders is one of the main observation methods. The EP-16 type electron-optical transducers with the electrostatic focusing allow us to obtain photographs of the plasma-flow profile with an exposure of about 10 ns. In addition, high-speed continuous-strip, photographic recorders SFER-6 were used [41].

Diagnostics by both methods demonstrated the compactness of the plasma formations in the case of propagation to distances considerably exceeding their transverse dimensions. This is indicative of exceeding the longitudinal velocity of the jet motion over its transverse expansion velocity. Figure 3 shows the flow-front photographs, which were obtained during the discharges in various gases and at various distances. The flow-structure dependence on the chemical composition of the working gas is observed, which seems to be related to the influence of the radiation cooling effects. The shock waves at the flow front are distinctly seen (an analog of the Herbig–Haro object). The head part of the flow has a transverse size of several centimeters even at large distances.

Operation during the stationary filling of the discharge chamber with working gas is a feature of the PF-3 experiment. After the plasma compression, the gas ionization by the X-ray radiation of the pinch is observed on the axis and the flow propagates in the partially ionized plasma. The ionization degree of the background gas is a function of a large variety of factors, in particular, the X-ray radiation output and the type of the working gas, which determines the radiation absorption. Obviously, the ionization degree is a function of the radiation-absorption length and varies depending on the distance to the radiation source.

Therefore, the parameters of the medium vary as the flow travels away from the generation point.

The experimental conditions allowed one to estimate the plasma parameters by the spectral methods at a distance no closer than 35 cm. According to [42], for a discharge in helium, the background-plasma concentration at this distance amounts to $N_i \approx 2 \cdot 10^{16}$ cm^{-3}, which corresponds to a 20% ionization of the initial gas. At the same time, the plasma density of the flow itself is by one order of magnitude greater and equals $N_\mathrm{i} \approx 2 \cdot 10^{17}\,\mathrm{cm}^{-3}$ and the flow-plasma temperature is about 5 eV.

Therefore, the conditions which are in terms of contrast close to those observed in the case of young stars are reached in the experiment. The environmental influence on the flow stability can be estimated in the course of a more detailed analysis. In particular, it is possible to vary the background-plasma parameters by creating the profiled gas distributions with the help of the pulsed gas supply [43]. Therefore, it is possible to simultaneously satisfy the optimal conditions for the working pressure in the insulator region and significantly vary the medium parameters in the flow-propagation region by varying the supply parameters.

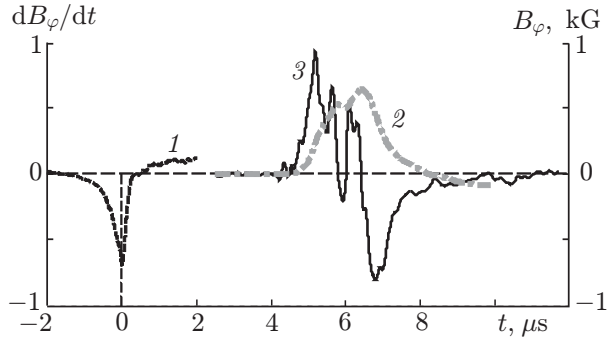

Fig. 4. The results of measuring the azimuthal magnetic fields for $z = 35$ cm, $r = 3$ cm (the gas is neon, the chamber pressure is $P_0 = 2.0$ torr, $U_0 = 9$ kV, and the energy input to the discharge is $W_0 = 373$ kJ): the time derivative of the total current (black dashed line *1*, in relative units). The azimuthal magnetic field (gray line *2*) and its derivative (solid line *3*).

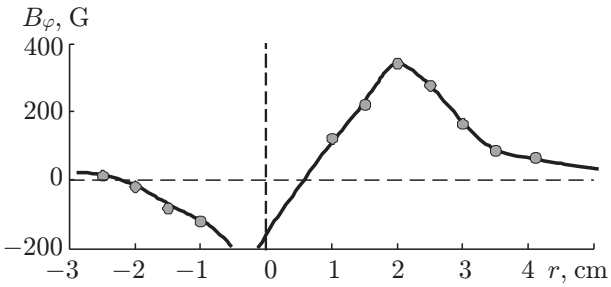

Fig. 5. Radial distribution of the azimuthal magnetic field in the plasma jet of the PF-3 facility at the height $z = 35$ cm from the anode surface. The chamber axis is shown by a vertical dashed line.

As was mentioned, the current and magnetic-field distributions in the flow are among the most interesting issues. Using the magnetic-sensing methods, it has been earlier [44] shown that the plasma flow propagates with the "frozen-in" magnetic field (see Fig. 4). The azimuthal magnetic-field component is considered to be the main one. In the experiments with the PF-3 facility, its value by an order of magnitude is 10^3 G at a distance of 35 cm. The longitudinal magnetic field along the motion direction is an order of magnitude smaller. Still stronger fields about 10 kGs were detected in the experiments using the Mather-type facility KPF-4 [45].

One of the important results of the above-mentioned works is that the observed radial distribution of the azimuthal magnetic field for the experimental conditions obtained using the PF-3 facility is readily explained by the longitudinal current about 10 kA flowing in the near-axial jet region. Therefore, two important conclusions are made. First, the estimates show that the magnetic field created by this current can be sufficient to ensure the Bennett equilibrium of the plasma. In this case, the stable-state duration of the jet should be determined by the time of decay of the currents circulating in the plasma. Second, if the axial current is present, it should be closed on the periphery.

The previously performed studies have been mainly directed at analyzing the field distribution in the paraxial region. It is shown that the field-behavior character for $r > r_\mathrm{core}$ is well described by the dependence $B \propto r^{-1}$ (see Fig. 5), which obviously agrees with theoretical models. However, in some cases where the flow axis was displaced with respect to the chamber axis, it was possible to study the features of the peripheral behavior of the field. In particular, according to the obtained data, the current "closing" radius exceeds 5 cm and, most probably, amounts to 6–7 cm.

Indeed the character of the field distribution at relatively large distances from the jet axis is a function of the backward-current distribution. In the case of a uniform current distribution when approaching the

backward current line, the magnetic field falls off at a higher rate tending to zero on the closure surface. In the experiment and, with high probability, under actual conditions, uniform homogeneous azimuthal distributions are not reached, i.e., the observed flow tends to channeling. In this case, the magnetic-probe signal is a function of its location with respect to the current channels. The examples of possible current distributions are discussed in [44].

Finally, it should be emphasized that since the magnetic-field sensors have fixed experimental locations and the current distribution is random, it is necessary to perform a sufficiently large series of experiments for obtaining the required statistical data in order to determine the basic laws of distribution of the currents flowing in the plasma stream.

As was noted, the relationship between the densities of the electromagnetic-field energy flux and kinetic energy of the particles is very important for determining the nature of a jet ejection. The available experimental potential allows one to estimate the kinetic energy of the flow with acceptable accuracy. To this end, one can primarily use the data on the flow velocity and density. Moreover, it is possible to directly measure the flow momentum and energy using the ballistic pendulum-calorimeter. Measuring the density of the electromagnetic-energy flux (the Poynting vector) is more difficult since the electric-field measurement in plasma is fraught with serious experimental problems.

Recording the azimuthal rotation of the flow can be an alternative. In this case, the direct measurements are also extremely difficult. According to the estimates, in the studied case, the Doppler shift is too small to isolate it against the background of large Stark broadening. Some indirect evidence testify to rotation of the current-carrying plasma envelope at the stage of the pinch formation, which, in particular, leads to the appearance of a longitudinal magnetic field [46]. This rotation can also add a rotational momentum to the plasma flow formed in the pinch. Evidence for the possible flow rotation is also found in the experiments using the measurements in which high-speed continuous-strip recorders were used for the measurements [41]. However, the available data is not sufficient for obtaining quantitative estimates of the rotation speed. The data on rotation of the magnetic-field vector can be considered to be the most reliable at this time [40, 44]. Under the conditions of the magnetic-field "freezing" into the plasma, this rotation can be related to the rotation of the plasma flow as a whole. It is assumed that these studies are among the main directions of our future activities.

4. DISCUSSION

To sum it up, it can be assumed that the plasma focus at its compression time, i.e., the pinch formation, creates a plasma flow along the facility axis with the following plasma parameters: the density is $N \gtrsim 10^{17}$ cm^{-3}, the electron and ion temperature is 1–5 eV, the plasma-ejection motion velocity is $v_{\parallel} \approx 5 \cdot 10^6$ cm/s, and, finally, the magnetic field frozen into the flow is $B \approx 10^2$–10^3 G. The azimuthal component B_φ is the main magnetic-field component. The longitudinal magnetic field B_z along the motion direction is an order of magnitude smaller. The azimuthal magnetic field is created by the electric field flowing in the paraxial region with a diameter of about 2–3 cm.

The total electric current flowing along the center creates the azimuthal magnetic field whose direction indicates that the electric-current density projection on the z axis, which is directed along the flow, is negative ($j_z < 0$). This confirms that the current is created by the electrons traveling in the positive direction along the z axis. Let us finally note that using Eqs. (2) and (7), one can obtain the estimate for the nonrelativistic magnetization parameter

$$\sigma_{\rm n} \sim \frac{W_{\rm tot}^{3/2}}{\dot{M}^{3/2} v_{\rm in}^3}, \tag{8}$$

which yields $\sigma_{\rm n} \sim$ 10–100. It is obvious that this key parameter turns out to be almost the same as that for the actual jet ejections.

The plasma ejection has the finite lifetime $\tau \approx$ 10–40 μs since it lacks the source to renew the energy loss because of its detachment from the "central machine." This means that, as it has been already

mentioned, the electric field, which creates electric current, is of inductive origin

$$\frac{\partial E_z}{\partial r} = \frac{1}{c}\frac{\partial B_\varphi}{\partial t}. \tag{9}$$

Here, c is the light speed in free space and t is the time. Introducing the isotropic conductance σ of the plasma in the simplest case, we obtain the equation of the magnetic-field diffusion:

$$\frac{\partial B_\varphi}{\partial t} = \frac{c^2}{4\pi\sigma}\Delta B_\varphi, \tag{10}$$

where Δ is the Laplace operator. Therefore, the magnetic-field decay time $\tau \approx 4\pi r^2\sigma/c^2 \approx 5 \times 10^{-6}$ s corresponds to the plasma-bunch lifetime. It is assumed that the plasma conductance is of the order of the classical Spritzer one, i.e., $\sigma \approx 10^{14}$ s^{-1}. The longitudinal electric field

$$E_z = \frac{c}{4\pi\sigma}\frac{1}{r}\frac{\partial}{\partial r}\left(rB_\varphi\right) \tag{11}$$

is observed in two regions, namely, the central region, where $E_z \approx rB_\varphi/(c\tau) \approx 3\,\mathrm{V/cm}$, and the periphery ($r \approx 10$ cm), where the magnetic field B_φ falls off faster than $1/r$. In this case, the projection E_z reverses sign and electric current flows in the direction opposite to the central current. Thus, the current closure in the ejection occurs.

Apart from exciting the longitudinal inductive electric field, there occurs generation of the radial polarization field $E_r \approx B_\varphi l/(c\tau) \approx 30\,\mathrm{V/cm}$, where $l \approx 20$ cm is the longitudinal dimension of the plasma ejection. In the presence of the longitudinal magnetic field B_z, the plasma should azimuthally rotate with the electric-drift velocity $v_\varphi = -cE_rB_z/B_\varphi^2 \approx \pm 10^5$ cm/s. It is assumed that $B_z \approx 10^{-1}B_\varphi \approx \pm 10^2$ G. Therefore, the plasma ejection should rotate in the azimuthal direction if the longitudinal magnetic field is created in the focus-compression process. Because of the strong transverse compression, even a weak initial magnetic field can be many times amplified (the mechanism proposed by A. D. Sakharov in 1957 [47] for generation of strong magnetic fields).

The ejection-stability issue is of importance. The plasma pressure in a jet can be estimated by the formula $P = NT \approx 5 \cdot 10^4\,\mathrm{dyne/cm^2} \approx 40$ torr. It is comparable with the magnetic-field pressure $B_\varphi^2/(8\pi) \approx 4 \cdot 10^4\,\mathrm{dyne/cm^2}$. This means that the magnetic field plays an important role in the transverse equilibrium of the ejection. The external gas pressure amounts to several torr, which is much smaller than the internal pressure of the plasma and the magnetic field. Therefore, the external gas pressure in a laboratory experiment can hardly resist the internal one. Moreover, the azimuthal magnetic field on the ejection periphery turns to zero after the electric-field closure.

Finally, the pressure gradient $\partial P/\partial r$ in the plasma located in the longitudinal magnetic field B_z initiates the azimuthal drift of the ions and electrons. Thus, a diamagnetic electric current appears. The drift velocity of electrons is equal to $v_\mathrm{d} = (\partial P/\partial r)/(m_eN\omega_\mathrm{ce})$, where ω_ce is the cyclotron frequency of electrons in the poloidal magnetic field B_z. Substituting the characteristic values to this expression, we obtain the estimate $v_\mathrm{d} \approx 2 \cdot 10^5$ cm/s. Obviously, the diamagnetic velocity amounts to about the electric-drift velocity $v_\mathrm{d} \approx v_\varphi$. Therefore, although the radial pressure of electrons can be compensated by the radial electric field, such a compensation is not provided for ions. In addition, to retain ions, an additional force ensuring the azimuthal rotation is required. The actual nature of the radial equilibrium of the jet is unknown, and this problem should be solved experimentally.

5. CONCLUSIONS

The PF-3 facility actually allows us to study the propagation, transverse structure, and stability of the nonrelativistic jet ejections. In this case, as was shown, many experimentally obtained key parameters, e.g., the magnetization parameter σ_n are in good agreement with those derived using the MHD models of

the actual jet ejections from the young stars.

In conclusion, let us again formulate the main astrophysical problems, which can be solved during the laboratory simulation of the jet ejections. First of all, we speak of the study of the internal jet structure. The hydrodynamic and electromagnetic forces acting on the plasma depend on the structure of the material flow in the jet. Within the framework of this problem, the relationships between the plasma motion, the electric-current generation by the moving charges, the magnetic-field structure, and formation of the volume forces, which again cause the plasma motion, are of great importance. It is noteworthy that since the magnetic field in the high-conductance plasma is entrained by the material, in the case of the complex plasma motion, one can expect the formation of a complex structure of the magnetic field.

It is also of interest to study the processes which occur if the system deviates from equilibrium. They can be of the oscillatory nature and, in particular, lead to the formation of the observed radiation. It is important to understand the factors which influence the velocity of approaching the equilibrium since this determines the jet-propagation regime and the proximity of this regime to the equilibrium or the stationary states. Therefore, the problem of stability of the jet ejections and, on the whole, their stationary nature deserves very careful attention.

The study of plasma ejections in laboratory experiments allows us to understand the structure and the cause of the collimation and stability of the jets despite their limited existence time. Special attention should be paid to the necessity of conducting studies with allowance for close connection among the astrophysical observations, the physical theory, and the laboratory experiment. The astrophysical observations allow us to snapshot the jet-ejection structure at some time, but prevent us from observing the entire process starting from the jet-initiation time. However, it is impossible to carry out the active space experiment since the state of the medium and other parameters characterizing the astrophysical plasma ejection cannot be changed. Although the spatial scales of the jet extension cannot be used in a laboratory experiment, it is possible to both observe the jet ejection from initiation to the disappearance time and change the experimental conditions and, thereby, study the system response to external action. The repeatability and reproducibility of the laboratory-experiment results are very important from the viewpoint of the problem of stability and stationarity of the jets.

This work is supported by the Russian Science Foundation (project No. 16–02–10051).

REFERENCES

1. C. Bertout, *Annu. Rev. Astron. Astrophys.*, **27**, 351 (1989).
2. J. Heyvaerts, *Plasma Astrophys.*, Springer, Berlin (1996).
3. G. Pelletier and R. Pudritz, *Astrophys. J.*, **394**, 117 (1992).
4. J. Woitas, F. Bacciotti, T. P. Ray, et al., *Astron. Astrophys.*, **432**, 149 (2005).
5. D. Coffey, F. Bacciotti, T. P. Ray. et al., *Astrophys. J.*, **663**, 350 (2007).
6. R. D. Blandford and D. R. Payne, *Mon. Not. R. Astron. Soc.*, **199**, 883 (1982).
7. C. Sauty and K. Tsinganos, *Astron. Astrophys.*, **287**, 893 (1994).
8. C. Sauty, E. Trussoni, and K. Tsinganos, *Astron. Astrophys.*, **421**, 797 (2004).
9. F. Shu, J. Najita, E. Ostriker, et al., *Astrophys. J.*, **429**, 781 (1994).
10. M. M. Romanova, G. V. Ustyugova, A. V. Koldoba, and R. V. E. Lovelace, *Mon. Not. R. Astron. Soc.*, **421**, 63 (2012).
11. R. Pudritz, M. J. Hardcastle, and D. C. Gabuzda, *Space Sci. Rev.*, **169**, 27 (2012).
12. C. Zanni and J. Ferreira, *Astron. Astrophys.*, **550**, 99 (2013).
13. S. Appl and M. Camenzind, *Astron. Astrophys.*, **256**, 354 (1992).

14. S. Appl and M. Camenzind, *Astron. Astrophys.*, **274**, 699 (1993).
15. V. S. Beskin and L. M. Malyshkin, *Astron. Lett.*, **26**, 208 (2000).
16. T. Lery, J. Heyvaerts, S. Appl, et al., *Astron. Astrophys.*, **337**, 603 (1998).
17. T. Lery, J. Heyvaerts, S. Appl, et al., *Astron. Astrophys.*, **347**, 1055 (1999).
18. D. Ryutov, R. P. Drake, J. Kane, et al., *Astrophys. J.*, **518**, 821 (1999).
19. D. D. Ryutov, M. S. Derzon, and M. K. Matzen, *Rev. Mod. Phys.*, **72**, 167 (2000).
20. D. D. Ryutov and B. A. Remington, *Plasma Phys. Controlled Fusion*, **44**, B407 (2002).
21. B. A. Remington, R. P. Drake, and D. D. Ryutov, *Rev. Mod. Phys.*, **78**, 75 (2006).
22. A. Ciardi, S. V. Lebedev, A. Frank, et al., *Astrophys. J. Lett.*, **691**, L147 (2009).
23. F. Suzuki-Vidal, S. V. Lebedev, S. N. Bland, et al., *IEEE Trans. Plasma Sci.*, **38**, 581 (2010).
24. F. Suzuki-Vidal, M. Bocchi, S. V. Lebedev, et al., *Phys. Plasmas*, **19**, 022708 (2012).
25. M. Huarte-Espinosa, A. Frank, and E. G. Blackman, *Astrophys. J.*, **757**, 66 (2012).
26. F. Suzuki-Vidal, S. V. Lebedev, M. Krishnan, et al., *High Ener. Dens. Phys.*, **9**, 141 (2013).
27. M. Huarte-Espinosa, A. Frank, E. G. Blackman, et al., *High Ener. Dens. Phys.*, **9**, 264 (2013).
28. B. Albertazzi, A. Ciardi, M. Nakatsutsumi, et al., *Science*, **346**, 325 (2014).
29. N. V. Filippov, T. I. Filippova, V. P. Vinogradov, *Nuclear Fusion: Supplement. Pt. 2*, 577 (1962).
30. D. Mourenas, J. Vierne, F. Simonet, et al., *Phys. Plasmas*, **10**, 605 (2003).
31. V. S. Beskin, *MHD Flows in Compact Astrophysical Objects*, Springer, Heidelberg (2010).
32. J. Contopoulos and R. V. E. Lovelace, *Astrophys. J.*, **429**, 139 (1994).
33. J. Heyvaerts and C. Norman, *Astrophys. J.*, **347**, 1055 (1989).
34. V. S. Beskin, *Physics–Uspekhi*, **40**, No. 7, 659 (1997).
35. S. V. Bogovalov, *Astron. Lett.*, **21**, 625 (1995).
36. T. Chiueh, Z. Li, and M. C. Begelman, *Astrophys. J.*, **377**, 462 (1991).
37. D. Eichler, *Astrophys. J.*, **419**, 111 (1993).
38. V. S. Beskin and E. E. Nokhrina, *Astron. Rep.*, **54**, 735 (2010).
39. V. Krauz, V. Myalton, V. Vinogradov, et al., *Phys. Scr.*, **2014**, 014036 (2014).
40. V. Krauz, V. Myalton, V. Vinogradov, et al., *42nd EPS Conf. Plasma Phys., Lisbon, Portugal, 22–26 June 2015. Vol. 39E, p. 4401.*
41. S. S. Ananyev, S. A. Dan'ko, V. V. Myalton, et al., *Vopr. Atom. Nauki Tekhn. Ser. Termoyad. Sint.*, **36**, No. 4, 102 (2013).
42. S. S. Ananyev, S. A. Dan'ko, V. V. Myalton, et al., *Plasma Phys. Rep.*, **42**, No. 3, 269 (2016).
43. D. A. Vojtenko, V. I. Krauz, S. S. Anan'ev, et al., *XLIIIth Int. (Zvenigorod) Conf. Plasma. Phys. Contr. Fusion, 8–12 Feb., 2016. Abstracts*, Plazmaiofan, Moscow (2016), p. 179.
44. K. N. Mitrofanov, V. I. Krauz, V. V. Myalton, et al., *J. Exp. Theor. Phys.*, **119**, No. 5, 910 (2014).
45. V. I. Krauz, D. A. Voytenko, K. N. Mitrofanov, et al., *Vopr. Atom. Nauki Tekhn. Ser. Termoyad. Sint.*, **38**, No. 2, 19 (2015).
46. V. I. Krauz, K. N. Mitrofanov, M. Scholz, et al., *Europhys. Lett.*, **98**, 45001 (2012).
47. A. D. Sakharov, *Sov. Phys. Usp.*, **9**, 294 (1966).